Optimal Substrate Shape for Vesicle Adhesion on a Curved Substrate

Wendong Shi[*,†], Xi-Qiao Feng[*] and Huajian Gao[†]

Abstract: When pulling a vesicle adhered on a substrate, both the force-displacement profile and the maximum force at pull-off are sensitively dependent upon the substrate shape. Here we consider the adhesion between a two-dimensional vesicle and a rigid substrate via long-range molecular interactions. For a given contact area, the theoretical pull-off force of the vesicle is obtained by multiplying the theoretical strength of adhesion and the contact area. It is shown that one may design an optimal substrate shape to achieve the theoretical pull-off force.

keyword: Biomechanics, Vesicle, Bio-adhesion, Adhesive contact, Optimal substrate shape

1 Introduction

Cell adhesion is one of the most important biological processes and also one of the most intensively studied areas of molecular and cellular biomechanics (1). Since lipid bilayer is the universal basis of cell membrane structure (2), vesicles composed of lipids provided a simplified model system for investigating mechanical properties of cell adhesion by excluding the effects of cytoskeleton and membrane proteins (3). Due to the fluidity of the membrane, the elastic deformation of membranes is mainly governed by the curvature elastic deformation (4, 5). Within the Canham-Helfrich curvature elasticity model, numerous theoretical models have been developed for both specific adhesion and nonspecific adhesion of vesicles (6–13). There have also been theoretical and experimental studies on pulling a vesicle initially adhered to a flat surface (14–22).

Recently, we have studied adhesion of a vesicle to a curved substrate via long-range molecular interactions and investigated how the substrate shape affects the adhesion strength (23). It was found that both the force-displacement profile and the maximum force at pull-off

---
[*] Department of Engineering Mechanics, Tsinghua University, Beijing 100084, P.R. China
[†] Division of Engineering, Brown University, 182 Hope Street, Providence, RI 02912

are sensitively dependent upon the substrate shape. This result indicates that probes with different tip shapes may be designed for cell manipulation. For example, a vesicle can be pulled off a flat surface using a probe with a curved tip. In the present paper, we calculate the optimal substrate shape which leads to the theoretically maximum pull-off force.
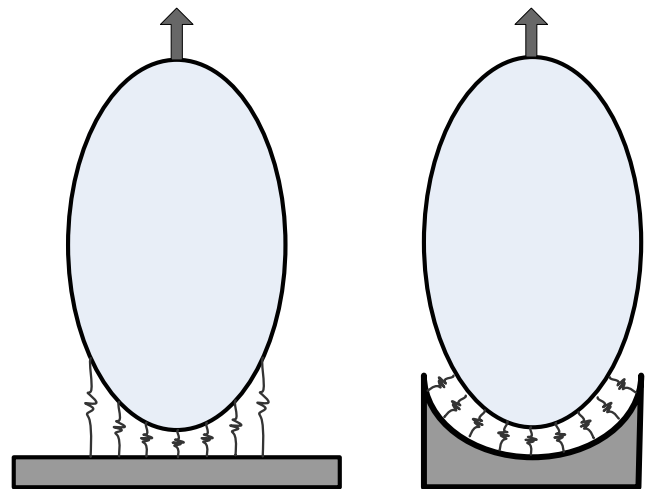
Figure 1 : (a) A vesicle adhered to a flat substrate and subjected to an external load. (b) A vesicle adhered to a curved substrate with the optimal shape (the springs represent the interaction forces between the vesicle and the substrate).

If two objects joined together by adhesion are subjected to an externally applied load, the pull-off process and the adhesion strength normally depend on the shape of the contact surfaces (24). Gao and Yao (25) have shown that there exists an optimal shape for the contact surfaces to achieve the maximum adhesion strength Σ_{th}. Such shape effects can be explained as follows. If a vesicle adhered to a planar substrate is subjected to an externally applied load, the adhesive force inside the contact area is nonuniform and normally only a small fraction of material bears effectively the applied pulling force at any instant in time, as shown in Fig. 1a. As the load increases, the

maximally stretched contact region ultimately reaches a critical stress and the adhesive joint would break via crack-like propagation. For the optimal shape, the vesicle and the substrate surfaces are spaced by a uniform separation over the entire contact region at pull-off, giving rise to a uniform stress field equal to the theoretical adhesive strength. In other words, if the two surfaces achieve perfect conformity at pull-off, as shown in Fig. 1b, the adhesion strength would reach the maximum value Σ_{th}. This article is aimed to demonstrate this effect for vesicles on curved substrates using a two-dimensional model.

2   Model

The optimal shape of the substrate is defined as such that a uniform distribution of normal stress equal to the theoretical strength Σ_{th} is achieved at pull-off of the vesicle. In what follows, we will calculate the shape of the vesicle at the critical moment of pull-off for optimal adhesion. The Young's modulus of a solid substrate is typically much higher than that of a vesicle and is therefore reasonably assumed to be rigid in the present paper (12).

We define the shape of the part of the vesicle subjected to the maximum allowable stress Σ_{th} as $Z_v(R)$. Following a similar argument made by Gao and Yao (25), the optimal shape of the substrate $Z_{so}(R)$ with a fixed adhesion area (e.g., a finite-sized probe) can be written as

$$Z_{so}(R) = Z_v(R). \tag{1}$$

The free energy of a vesicle subjected to a uniform distribution of stress Σ_{th} from S_1 to S_2 can be written as

$$F_{TOT} = \oint \left[\frac{\kappa_B}{2} (2M - 2M_0)^2 + \kappa_G K \right] dS$$
$$+ \Delta PV + \Gamma S + \int_{S_1}^{S_2} \Sigma_{th} Z \, dS \tag{2}$$

where the first integral term corresponds to the elastic bending energy of the membrane (4, 5); $M = (C_1 + C_2)/2$ is the mean curvature of the membrane with C_1 and C_2 being the principal curvatures, $K = C_1 C_2$ is the Gaussian curvature, M_0 is the mean spontaneous curvature induced by the asymmetry of the membrane bilayer, and κ_B and κ_G are the bending modulus and Gaussian rigidity, respectively. The second term in Eq. (2) is the free energy due to a pressure difference across the membrane, V is the vesicle volume, and ΔP can be regarded as a

Lagrange multiplier if the volume is assumed constant (26, 27). The third term in Eq. (2) can be regarded as the surface energy of membrane, with S being the surface area of the vesicle and Γ being the surface energy per unit area; Γ serves as the Lagrange multiplier to impose the constraint of a constant membrane area when the in-plane deformation of the membrane is neglected compared to the out-of-plane bending (26, 27). The last term in Eq. (2) represents the potential energy of the pulling stress Σ_{th} at the displaced position Z of the vesicle and the contact area is $S_2 - S_1$.

In the two-dimensional model, the free energy expression in Eq. (2) is reduced to

$$F_{TOT} = \frac{\kappa_B}{\rho} \left[\int_0^{2\pi} \frac{1}{2} (c(s) - c_0)^2 ds + \frac{p}{\rho^2} A + \int_{s_1}^{s_2} \sigma_{th} z \, ds \right] \tag{3}$$

where a constant contour length of the vesicle is assumed, A denotes the area of the 2D vesicle. The parameter $\rho = L/2\pi = $ constant is introduced as a normalizing length unit (8), and thereby, $ds = dS/\rho$, $c(s) \equiv 2M\rho$, $c_0 \equiv 2M_0\rho$, $p \equiv \Delta P \rho^3/\kappa_B$, $\sigma_{th} \equiv \Sigma_{th} \rho^3/\kappa_B$ and $z \equiv Z/\rho$ (23).
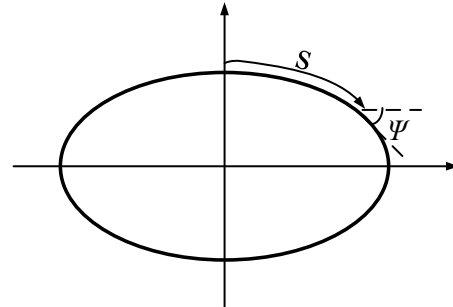
Figure 2 : Parametrization of the shape of a two-dimensional vesicle.

Using the arc length s as the basic coordinate, the shape of the vesicle can be described by the tangent function $\psi(s)$ or by coordinate functions $r(s)$ and $z(s)$ along the arc length, as shown in Fig. 2. In this system, the free energy can be written as

$$\frac{F_{TOT}}{2\kappa_B/\rho} = \int_0^\pi \left[\frac{1}{2} (\dot{\psi} - c_0)^2 + pz \cos\psi + \lambda(\dot{r} - \cos\psi) \right.$$
$$\left. + \chi(\dot{z} + \sin\psi) \right] ds + \int_{s_1}^\pi \sigma_{th} z \, ds. \tag{4}$$

The variation of the free energy function in Eq. (4) leads to

$$\delta\left(\frac{F_{\text{TOT}}}{2\kappa_B/\rho}\right) = \int_0^{s_1} [(-\ddot{\psi} - pz\sin\psi + \lambda\sin\psi + \chi\cos\psi)\,\delta\psi$$
$$+ \left(-\dot{\lambda}\right)\delta r + (-\dot{\chi} + p\cos\psi)\,\delta z + (\dot{r} - \cos\psi)\,\delta\lambda$$
$$+ (\dot{z} + \sin\psi)\,\delta\chi]\,ds$$
$$+ \int_{s_1}^{\pi} [(-\ddot{\psi} - pz\sin\psi + \lambda\sin\psi + \chi\cos\psi)\,\delta\psi$$
$$+ \left(-\dot{\lambda}\right)\delta r + (-\dot{\chi} + p\cos\psi + \sigma_{th})\,\delta z$$
$$+ (\dot{r} - \cos\psi)\,\delta\lambda + (\dot{z} + \sin\psi)\,\delta\chi]\,ds$$
$$+ [(\dot{\psi} - c_0)\,\delta\psi + \lambda\delta r + \chi\delta z]_{s=0}^{s=s_1}$$
$$+ [(\dot{\psi} - c_0)\,\delta\psi + \lambda\delta r + \chi\delta z]_{s=s_1}^{s=\pi}. \qquad (5)$$

Since the functions $\delta\psi(s_1)$, $\delta(s_1)$ and $\delta(s_1)$ are arbitrary, one obtains from Eq. (5) that

$$\dot{\psi}_+ = \dot{\psi}_-, \qquad (6a)$$

$$\dot{\lambda}_+ = \dot{\lambda}_-, \qquad (6b)$$

$$\dot{\chi}_+ = \dot{\chi}_- \qquad (6c)$$

where $\dot{\psi}_+$, $\dot{\lambda}_+$, $\dot{\chi}_+$ and, $\dot{\psi}_-$, $\dot{\lambda}_-$, $\dot{\chi}_-$ denote the values of the corresponding parameters at the starting and the end points of the arc length s_1, respectively. Here the continuities of

$$\psi_+ = \psi_-, \qquad (6d)$$

$$r_+ = r_-, \qquad (6e)$$

$$z_+ = z_- \qquad (6f)$$

have been assumed since the membrane has a continuous bilayer structure at s_1(28).

Using Eq. (5), we obtain the Euler-Lagrange equations corresponding to Eq. (4), which can be expressed in a system of first order ordinary differential equations:

$$\begin{cases} \dot{\psi} = u \\ \dot{u} = -pz\sin\psi + \lambda\sin\psi + \chi\cos\psi \\ \dot{\lambda} = 0 \\ \dot{\chi} = p\cos\psi \\ \dot{r} = \cos\psi \\ \dot{z} = -\sin\psi \end{cases} \quad (0 \le s \le s_1)(7a)$$

and

$$\begin{cases} \dot{\psi} = u \\ \dot{u} = -pz\sin\psi + \lambda\sin\psi + \chi\cos\psi \\ \dot{\lambda} = 0 \\ \dot{\chi} = p\cos\psi + \sigma_{th} \\ \dot{r} = \cos\psi \\ \dot{z} = -\sin\psi \end{cases} \quad (s_1 < s \le \pi)(7b)$$

The geometric boundary conditions are

$$\psi(0) = 0, \qquad (8a)$$

$$r(0) = 0, \qquad (8b)$$

$$\psi(\pi) = \pi, \qquad (8c)$$

$$r(\pi) = 0 \qquad (8d)$$

and additional boundary conditions can be obtained from the variational equation (5)

$$z(0) = z_0, \qquad (8e)$$

$$\chi(\pi) = 0. \qquad (8f)$$

3 Results

The shape function of the vesicle can be numerically determined by solving the governing equations (7a, b) together with the continuity conditions (6a–f) and the boundary conditions (8a–f). The deformed shapes of the vesicle are numerically solved by the shooting method and plotted in Fig. 3 (the solid contour) for parameter values $\sigma_{th} = 11.2$, $p \equiv 0$ and two normalized contact areas (1) $s_2 - s_1 = \pi/6$, (2) $s_2 - s_1 = \pi/3$. For comparison, the undeformed shape of the vesicle (the dashed contour) is also shown. The deformation of the vesicle is larger for the case of a larger contact area ($\pi/3$ as shown in Fig. 3) than for that of a smaller contact area ($\pi/6$ as shown in Fig. 3). Once the shape of the part of the vesicle subjected to Σ_{th} is calculated, the optimal shape of the substrate can be determined from the principle of perfect conformity at pull-off (25), via Eq. (1) for a fixed contact area (e.g., a finite-sized probe). Fig. 3 illustrates that the

Figure 3 : The undeformed (dashed contour) and deformed (solid contour) shapes of a vesicle under uniform stress $\sigma_{th} = 11.2$ for different contact areas ($s_2 - s_1 = \pi/6$ and $s_2 - s_1 = \pi/3$) with zero pressure difference ($p = 0$) across the membrane. According to the principle of perfect conformity at pull-off (25), the shape of the part of the vesicle under uniform stress $\sigma_{th} = 11.2$ is the optimal shape for a substrate to achieve theoretically maximum pull-off force with the vesicle if the contact area is fixed (e.g. a finite sized probe).

optimal shape of the substrate changes with the area of contact (i.e. the size of a probe).

The pressure difference p across the membrane can also have significant effects on the optimal shape of the substrate. When p exceeds a critical value ($\sim$3), a free standing circular vesicle becomes unstable against membrane buckling (8). Here we only consider cases when a free standing circular vesicle is still stable. Fig. 4 plots the undeformed (dashed contour) and deformed (solid contour) vesicle shapes when a uniform stress $\sigma_{th} = 11.2$ is applied over a fixed contact area $s_2 - s_1 = \pi/6$ under three values of the pressure difference: (1) $p = 0$, (2) $p = 1$, (3) $p = -1$. It is observed that the vesicle deformation increases with p, which can be easily understood as follows. A negative pressure difference indicates that the pressure in the interior of the vesicle has exceeded the pressure in the external environment. In this case, the membrane tension is increased by the pressure difference and the vesicle becomes more stiff. On the other hand, a positive pressure difference corresponds to the
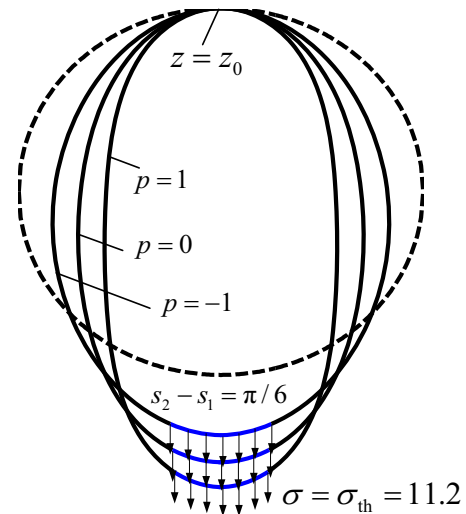
Figure 4 : The undeformed (dashed contour) and deformed (solid contour) shapes of a vesicle under uniform stress $\sigma_{th} = 11.2$ for different pressure differences ($p = -1, 0, 1$) between the interior and exterior environments of the vesicle under a fixed contact area $s_2 - s_1 = \pi/6$. A negative pressure difference corresponds to the case of internal pressure larger than external pressure.

external pressure exceeding internal pressure, in which case the effect of pressure is to decrease the tension in the membrane and to decrease the rigidity of the vesicle against deformation. These results indicate that the optimal shape of the substrate is also influenced by pressure differences in the environment of a vesicle

4   Summary

In summary, a variational approach has been adopted in this paper to calculate the optimal substrate shape to achieve the theoretical pull-off force for vesicle adhesion on a curved substrate. The present model may provide some guidelines for designing the devices of cell manipulation. Naturally, the optimal shape of the substrate depends on the adhesion strength between a vesicle and a surface. The concept developed in this article should be of general interest for understanding of vesicle-substrate adhesion.

References

1. Zhu, C., Bao, G. & Wang, N. (2000) *Annu. Rev. Biomed. Eng.* **2**, 189–226.

2. Alberts, B., Johnson, A., Lewis, J., Raff, M., Roberts, K. & Walter, P. (2002) *Molecular Biology of the Cell* (Garland, New York).

3. Lipowsky, R. (1998) In: Trigg, F. L. (ed) *Encyclopedia of applied physics* (WCH publishers, Weiheim and New York), 199–222.

4. Canham, P. B. (1970) *J. Theor. Biol.* **26**, 61–81.

5. Helfrich, W. (1973) *Z. Naturforsch. C* **28**, 693–703.

6. Seifert, U. & Lipowsky, R. (1990) *Phys. Rev. A* **42**, 4768–4771.

7. Lipowsky, R. (1991) *Nature* **349**, 475–481.

8. Seifert, U. (1991) *Phys. Rev. A* **43**, 6803–6814.

9. Seifert, U. (1997) *Adv. Phys.* **46**, 13–137.

10. Seifert, U. (1999) *Phys. Rev. Lett.* **83**, 876–879.

11. Brochard-Wyart, F. & de Gennes, P. G. (2002) *Proc. Natl. Acad. Sci. USA* **99**, 7854–7859.

12. Freund, L. B. & Lin, Y. (2004) *J. Mech. Phys. Solids* **52**, 2455–2472.

13. Shenoy, V. B. & Freund, L. B. (2005) *Proc. Nat. Acad. Sci.* **102**, 3213–3218.

14. Evans, E., Bowman, H., Leung, A., Needham D. & Tirrell, D. (1996) *Science* **273**, 933–935.

15. Heinrich, V., Bozic, B., Svetina, S. & Zeks, B. (1999) *Biophys. J.* **76**, 2056–2071.

16. Rosso, R. & Virga, E. G. (2000) *J. Phys. A: Math. Gen.* **33**, 1459-1464.

17. Guttenberg, Z., Bausch, A. R., Hu, B., Bruinsma, R., Moroder, L. & Sackmann, E. (2000) *Langmuir*, **14**, 8984–8993.

18. Boulbitch, A. (2002) *Europhys. Lett.* **59**, 910–915.

19. Boulbitch, A. (2003) *Eur. biophys. J. Biophys. Lett.* **31**, 637–642.

20. Smith, A. S., Sackmann, E. & Seifert, U. (2003) *Europhys. Lett.* **64**, 281–287.

21. Smith, A. S., Sackmann, E. & Seifert, U. (2004) *Phys. Rev. Lett.* **92**, 208101-1–208101-4.

22. Pierrat, S., Brochard-Wyart, F. & Nassop, P. (2004) *Biophys. J.* **87**, 2855–2869.

23. Shi, W. D., Feng, X. Q. & Gao, H. J. (2006) *Acta Mech. Sin.* **22**, 529-535.

24. Spolenak, R., Gorb, S., Gao, H. & Arzt, E. (2005) *Proc. R. Soc. London A* **461**, 305–319.

25. Gao, H. & Yao, H. (2004) *Proc. Natl. Acad. Sci. USA* **101**, 7851–7856.

26. Ou-Yang, Z. C. & Helfrich, W. (1987) *Phys. Rev. Lett.* **59**, 2486–2488.

27. Ou-Yang, Z. C. & Helfrich, W. (1989) *Phys. Rev. A* **39**, 5280–5288.

28. Julicher, F. & Lipowsky, R. (1996) *Phys. Rev. E* **53**, 2670–2683.